Determining the topological charge of an obstructed vortex beam via reconstructed phase distribution

Li, Xiaofei; Ma, Liqi; Zeng, Jun; Dong, Zhen; Liu, Lin; Wang, Fei; Hoenders, Bernhard J.; Cai, Yangjian; Liu, Xianlong

Published in:
Applied Physics Letters

DOI:
10.1063/5.0031147

Applied Physics Letters

Determining the topological charge of an obstructed vortex beam via reconstructed phase distribution

Cite as: Appl. Phys. Lett. **117**, 251103 (2020); https://doi.org/10.1063/5.0031147
Submitted: 28 September 2020 • Accepted: 10 December 2020 • Published Online: 22 December 2020

Xiaofei Li, Liqi Ma, Jun Zeng, et al.

Determining the topological charge of an obstructed vortex beam via reconstructed phase distribution

Cite as: Appl. Phys. Lett. **117**, 251103 (2020); doi: 10.1063/5.0031147
Submitted: 28 September 2020 · Accepted: 10 December 2020 ·
Published Online: 22 December 2020

Xiaofei Li,[1,2] Liqi Ma,[1,2] Jun Zeng,[3] Zhen Dong,[1,2] Lin Liu,[3] Fei Wang,[3] Bernhard J. Hoenders,[4,a)] Yangjian Cai,[1,2,3,a)] and Xianlong Liu[1,2,a)]

AFFILIATIONS

[1]Shandong Provincial Engineering and Technical Center of Light Manipulation and Shandong Provincial Key Laboratory of Optics and Photonic Devices, School of Physics and Electronics, Shandong Normal University, Jinan 250014, China
[2]Collaborative Innovation Center of Light Manipulations and Applications, Shandong Normal University, Jinan 250358, China
[3]School of Physical Science and Technology, Soochow University, Suzhou 215006, China
[4]Zernike Institute for Advanced Materials, University of Groningen, Nijenborgh 4, NL-9747 AG Groningen, The Netherlands

[a)]Authors to whom correspondence should be addressed: b.j.hoenders@rug.nl; yangjiancai@suda.edu.cn; and xianlongliu@sdnu.edu.cn

ABSTRACT

Determination of the topological charge (TC) of a vortex beam is of significant importance in various applications such as high-capacity optical communications and micromanipulations. Though many kinds of methods, until now, have been proposed to measure the TC, most of them will fail if the measured vortex beam is partially blocked by an opaque obstacle. In this Letter, we have introduced an efficient method to determine the TC of an incomplete vortex beam (partially blocked by an obstacle) using its reconstructed phase distribution under propagation. The numerical and experimental results showed that the sign and magnitude of the TC can be simultaneously determined by counting the number of phase singularities and the directions of the phase variations around the singularities occurring in the reconstructed phase pattern, respectively. Our method works even when half of the vortex beam is blocked.

A vortex beam, which possesses a helical wavefront $\exp(il\phi)$, has an orbital angular momentum (OAM) of $l\hbar$ per photon, where l is the topological charge (TC), ϕ is the azimuthal angle, and $\hbar$ is the Planck constant divided by 2π.[1] Owing to that OAM modes with different TCs compose an infinite number of orthonormal states in Hilbert space, space division multiplexing technology based on the OAM modes displays great potential for high-data rate information transfer in optical communications.[2,3] Hence, vortex beams have received considerable attention and have found diverse applications in super-resolution imaging,[4] optical trapping,[5,6] astronomy,[7] etc. In some applications, especially in OAM-based optical communications,[2,3] the accurate measurement of both the magnitude and sign of the TC is one of the key tasks. Therefore, one has to explore simple and effective methods to determine the TC of the vortex beam.

In recent years, various methods have been proposed to determine the TC of vortex beams.[8–33] Most of them are based on the intensity measurement such as interference methods,[8–11] diffraction methods,[12–14] and mode converters.[15,16] An extensive range of diffracting elements are used, such as gratings,[17–19] apertures,[20] and interferometers.[9] These methods are devoted to transforming different OAM modes into distinguishable intensity patterns in which one can determine the TC of the vortex beams. However, these methods will be unfeasible when the measured vortex beams are partially blocked by an opaque obstacle. In addition, several methods that are based on the complex spectrum measurement require complicated calculations and are impractical for real applications.[21,22] In addition, the phase measurement method is also another alternative way to determine the TC and has been widely studied in the previous papers,[23–26] e.g., a multi-pinhole plate phase determination method.[23]

On the other hand, it is inevitable in practical applications when a vortex beam is obstructed by obstacles during propagation, such as the suspended particles in free-space optical transmission and bubbles in underwater wireless optical communications.[34–37] One of the effective methods is using an Airy beam to evade obstacles for its self-bending property.[35] However, when the beam is obstructed during propagation, it will be a great challenge to determine its TC for its incomplete intensity. Hence, beams with self-healing properties or with self-reconstruction abilities have been widely investigated.[36,37] The non-diffracting beams, e.g., Bessel beams,[38] and Mathieu beams[39] possess the marvelous property of reconstruction,[40] which means that the beam could reconstruct its original structure through propagation when it is partially obstructed by an obstacle. The reconstruction phenomenon attracts widespread attention because not only the intensity but also the degree of coherence and polarization of the beam could self-reconstruct during propagation.[41–44] It was revealed that even the Laguerre-Gaussian beams (not belonging to non-diffracting beams) have a certain seal-healing ability during propagation.[45] Can we determine the TC from the reconstructed intensity or phase of vortex beams?

Here, we study the transmission evolution of a Gaussian vortex beam after being obstructed by a sector-shaped opaque obstacle and establish the relationship between the phase singularities and the TC from the reconstructed phase distribution. Based on the established relationship, we proposed an efficient approach to simultaneously measure the magnitude and sign of the partially obstructed vortex beams. The experimental results agree well with the simulation results. Our finds will be helpful in OAM multiplexing communications.

We start from the electric field of a typical vortex beam, i.e., a Gaussian vortex beam. The electric field in the source plane can be expressed as[31]

$$E_s(r,\phi,0) = \exp\left(-\frac{r^2}{w_0^2}\right)\exp(il\phi), \tag{1}$$

where r and ϕ denote the radial and azimuthal coordinates, respectively, w_0 is the beam waist radius, and l is the TC.

In some practical situations, the vortex beam may inevitably encounter obstacles in an optical path. The amplitude and phase are disturbed by the obstacles. In order to investigate the intensity and phase evolution of the incomplete vortex beam, here, we suppose that the vortex beam is obstructed by a sector-shaped opaque obstacle (SSOO) with center angle α, of which the transmission function $T(\phi)(-\alpha/2 < \phi < \alpha/2)$ within the area of angle α equals zero; otherwise, $T(\phi) = 1$. Under this circumstance, the electric field of the vortex beam through a stigmatic ABCD system can be evaluated by the Collins integral,[46]

$$E_r(\rho,\theta,z) = \frac{-ik}{2\pi B}\int_0^\infty\int_{\alpha/2}^{2\pi-\alpha/2} E_s(r,\phi,0) \times \exp\left\{\frac{ik}{2B}\left[Ar^2 + D\rho^2 - 2\rho r\cos(\theta-\phi)\right]\right\} r\,dr\,d\phi, \tag{2}$$

where ρ and θ denote the radial and azimuthal coordinates in the output plane, respectively. $k = 2\pi/\lambda$ is the wave number with λ being the wavelength of the incident field. A, B, and D are the transfer matrix elements of the stigmatic ABCD optical system. Note that in Eq. (3), the integrating over azimuthal angle is from $\alpha/2$ to $2\pi - \alpha/2$ due to the effect of the SSOO.

Let us pay attention to the propagation characteristics of the obstructed Gaussian vortex beam in a focusing system. A thin lens with focal length f is placed in the source plane, and the receiver plane is located at a distance z from the thin lens, see Fig. 5. The transfer matrix of the optical system then can be calculated as

$$\begin{pmatrix} A & B \\ C & D \end{pmatrix} = \begin{pmatrix} 1 & z \\ 0 & 1 \end{pmatrix}\begin{pmatrix} 1 & 0 \\ -1/f & 1 \end{pmatrix} = \begin{pmatrix} 1-z/f & z \\ -1/f & 1 \end{pmatrix}. \tag{3}$$

Substituting Eq. (3) into Eq. (2), one can study the propagation properties of the obstructed beam, e.g., the intensity evolution, which can be expressed as

$$I_r(\rho,\theta,z) = |E_r(\rho,\theta,z)|^2, \tag{4}$$

and its transverse power flow can be calculated from the Poynting vector, which is expressed as[1]

$$\vec{S}_\perp = \vec{S}_x + \vec{S}_y = \frac{-i}{4\eta_0 k}E^*\vec{\nabla}_\perp E. \tag{5}$$

By using the expanded expressions of the sector shape,[47] one could derive the analytical expressions of the obstructed vortex beam during propagation. For simplicity, we only show the simulation results.

Figure 1 shows the density plots of the normalized intensities and their transverse power flow distributions (see the arrows) of a focused Gaussian vortex beam with $l = 4$ and $f = 150$ mm. We present the examples with the SSOO $\alpha = 0°, 90°, 180°$, respectively, and study the performance for different propagation distances z. One can infer from Fig. 1 that the intensity of a Gaussian vortex beam is rotating during propagation due to the effect of the vortex phase, a rotation of 90° from the source to the far-field plane (focal plane), see Figs. 1(a-2)–1(d-2) and 1(a-3)–1(d-3). It can also be seen from Fig. 1 that the intensity distribution cannot be well reconstructed when the vortex beam is partially blocked by the SSOO.

However, the rotation of the intensity pattern could be much more clearly understood from its transverse power flows $\vec{S}_\perp$. The transverse power flows $|\vec{S}_\perp|$ display a vortex structure due to the existence of the spiral phase when there are no obstacles in the source plane, see Figs. 1(a-1)–1(d-1). When the beam is obstructed by the SSOO, the energy flows into the obstructed area from the opposite side, e.g., from the top to the bottom side, see Figs. 1(d-2) and 1(d-3). We should emphasize here that if the sign of TC is negative, the direction of transverse energy flows during propagation is reversed. As a result, the dark area of the intensity pattern in the focal plane is at the bottom side, not at the top side shown in Figs. 1(d-2) and 1(d-3). Therefore, the sign of the TC can be determined from the rotation direction of the incomplete intensity pattern.

However, we notice that the intensity properties show nothing about the magnitude of the TC even when the beam has not been obstructed. Therefore, how can we determine the TC of the obstructed vortex beam? One convenient approach is to recover the magnitude of the TC just performing the Fourier transform of the far-field intensity.[32] The number of dark rings of the Fourier transform pattern is just equal to the number of TCs. To demonstrate the feasibility of this approach under the condition of incomplete intensity, the Fourier transform of the far-field intensity distribution is numerically evaluated using the following integral:[32]

$$F_r(\nu,\varphi,z) = \int_0^\infty\int_0^{2\pi} I_r(\rho,\theta,z)\exp\{-i2\pi\nu\rho\cos(\theta-\varphi)\}\rho\,d\rho\,d\theta. \tag{6}$$

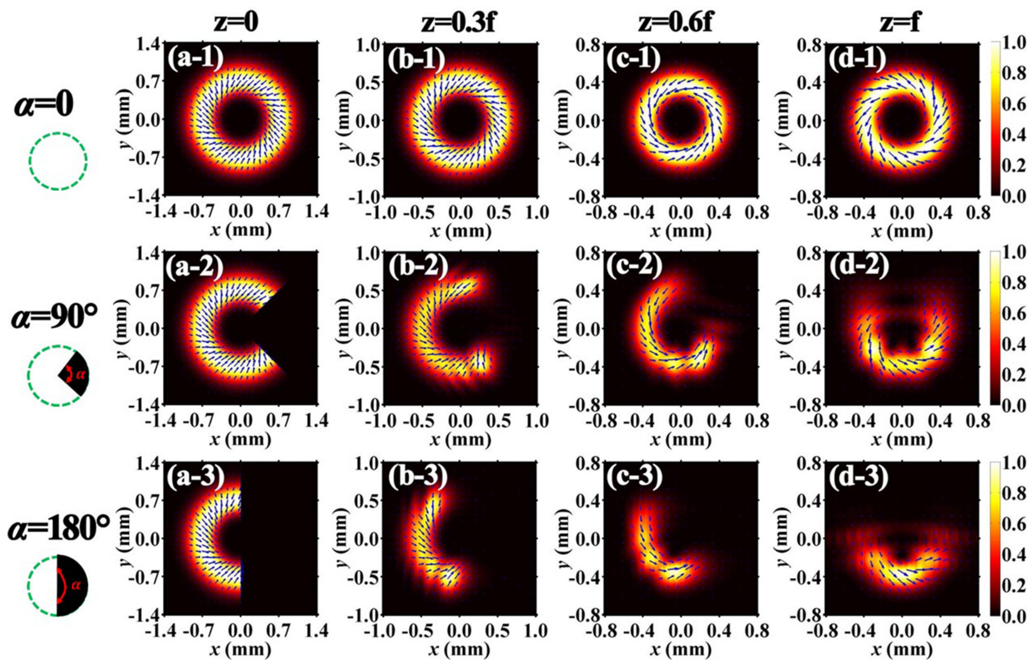

FIG. 1. Density plots of the normalized intensities and their transverse power flow distributions of a focused Gaussian vortex beam with $l = 4$ and $f = 150$ mm, obstructed by a SSOO with center angles $\alpha = 0^\circ$ [(a-1)–(d-1)], $\alpha = 90^\circ$ [(a-2)–(d-2)], and $\alpha = 180^\circ$ [(a-3)–(d-3)], respectively, for different propagation distances z.

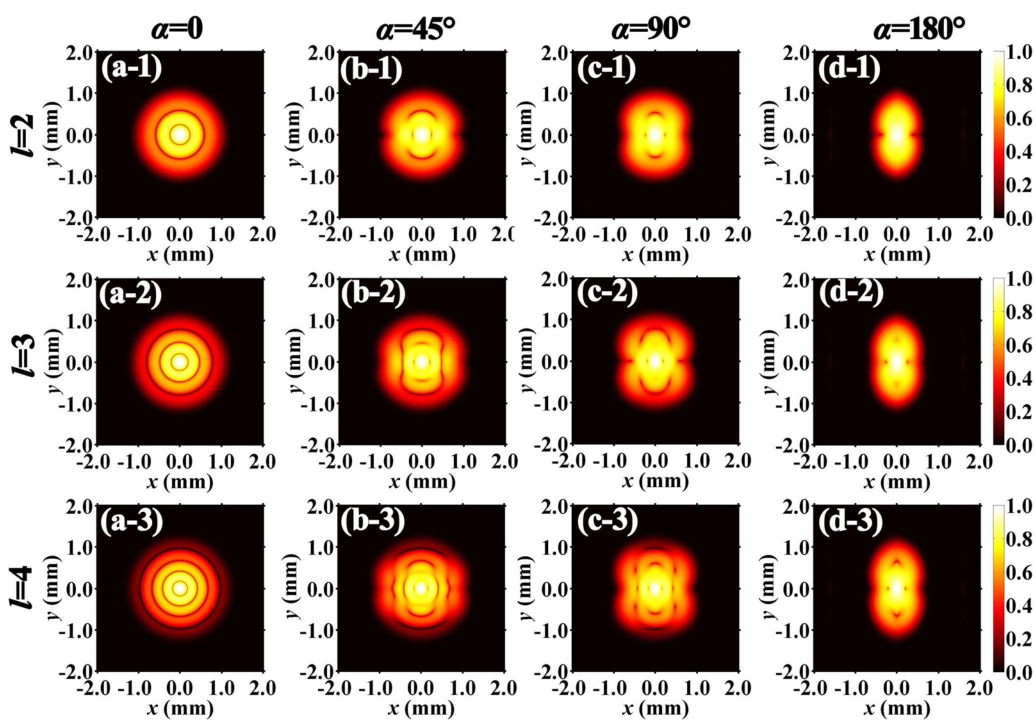

FIG. 2. Density plots of the normalized Fourier transform patterns of the Gaussian vortex beam in the focal plane with $f = 150$ mm, after being obstructed by different SSOOs with the TC $l = 2$ [(a-1)–(d-1)], $l = 3$ [(a-2)–(d-2)], and $l = 4$ [(a-3)–(d-3)], for different center angles α, respectively.

Figure 2 illustrates the normalized Fourier transform patterns of the far-field intensity (in the focal plane) with different TCs $l = 2$, 3, 4, respectively. When the vortex beam is not blocked ($\alpha = 0$), the number of dark rings equals the magnitude of the TC, as expected. However, the approach does not work as the angle of the SSOO increases. The Fourier transform patterns with different TCs are almost the same if half of the vortex beam is blocked ($\alpha = 180°$) and, therefore, no information about the TC can be obtained. We also investigated the effectiveness of other methods based on the intensity measurement[48–52] and found that these methods failed to determine the TC when half of the beam is blocked.

In order to determine the TC of a vortex beam from its incomplete intensity distribution, here, we propose a method whereby, using the reconstructed phase of the vortex beam, information about the TC can be obtained. The phase distribution of the complex electric field is calculated from the formula $\Phi = Arg[E_r(\rho, \theta, z)]$, where Arg denotes the phase angle of the electric field. Figure 3 presents the numerical results of the phase evolutions of the obstructed Gaussian vortex beam with TC being $l = 4$. Without the SSOO [see in Figs. 3(a-1)–3(d-1)], the phase singularity keeps the propagation axis unchanged. The varying of phase from $-\pi$ to π (or from 0 to 2π) four times along the closed loop in the clockwise direction around the phase singularity. The varying times and varying directions correspond to the magnitude and sign of the TC, respectively. When the beam has been obstructed by a SSOO, the evolution of the phase singularity is quite different. As shown in Figs. 3(a-2)–3(d-3), the single phase singularity splits into several ones during propagation. For each phase singularity, the varying of the phase around the singularity is from $-\pi$ to π (+1 TC). Interestingly, it is found that the number of phase singularities equals the magnitude of the TC from the far-field phase distribution [see Figs. 3(a-2)–3(d-2) and 3(a-3)–3(d-3); the black circles depict the position of the phase singularities.]. In addition, the sign of the TC corresponds to the phase varying direction around each split singularity. Therefore, the magnitude and the sign of the TC are determined from the reconstructed phase in the far field.

The physical mechanism behind this phenomenon is that the TC is a conserved quantity in a wave field, and the optical vortices can be created and annihilated only in pairs of opposing charge. When the vortex beam interacts with amplitude-only obstacles, there is no OAM transfer in the process, i.e., the OAM for each photon of the transmitted beam is still $l\hbar$. As a consequence, the TC information hidden in the reconstructed phase distribution will be recovered with the help of diffraction effects, i.e., propagation of a certain distance from the source plane. In practical applications, it is a convenient way to measure the TC from the far-field reconstructed phase distribution due to that the phase distribution is relatively stable and is easy to produce with the help of a thin focal lens. Remarkably, our approach works even when half of the beam is blocked [see in Fig. 3(d-3)].

To verify the corresponding relationship between the TC and the number of phase singularities of the light field in the far field, we plot in Fig. 4 the numerical results of the phase distributions of the obstructed Gaussian vortex beams with different TCs $l = \pm 2, \pm 4$ in the focal plane. It can be seen that the number of phase singularities is always equal to the magnitude of the TC and the sign of the TC still corresponds to the phase varying direction around singularities, regardless of the opaque angle of the SSOO, which indicates the accuracy and effectiveness of our method to measure the TC of the partially blocked vortex beams.

Now, we carry out experiments to demonstrate the determination method for the TC of a vortex beam obstructed by a SSOO from the reconstructed phase distribution. Our experimental setup is shown in Fig. 5. A diode-pumped solid-state linear polarized laser beam with

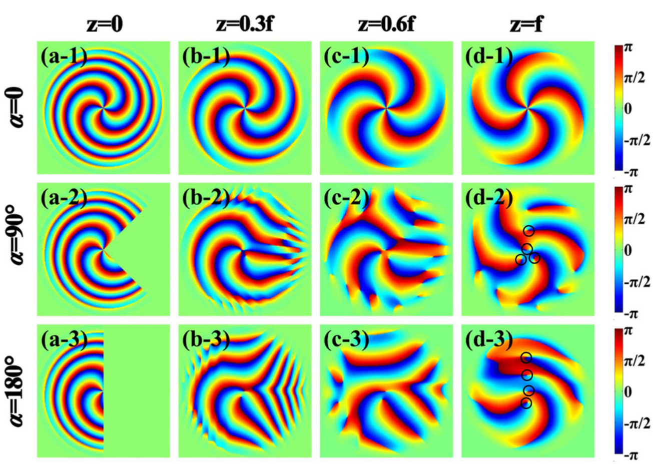

FIG. 3. Density plots of the phase distribution of the focused Gaussian vortex beam with $l = 4$ and $f = 150$ mm, obstructed by a SSOO with center angle $\alpha = 0°$ [(a-1)–(d-1)], $\alpha = 90°$ [(a-2)–(d-2)], and $\alpha = 180°$ [(a-3)–(d-3)], respectively, for different propagation distances z; the solid circle represents the phase singularity with $l = 1$.

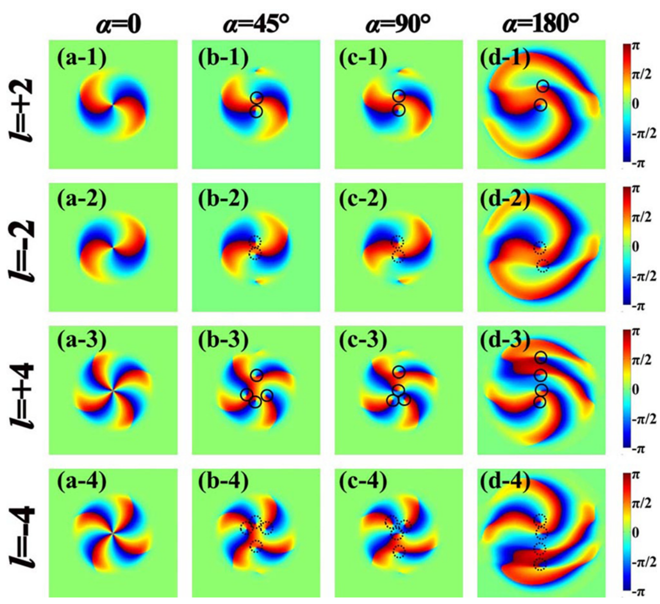

FIG. 4. Density plots of the phase distribution of the Gaussian vortex beam with $f = 150$ mm obstructed by a SSOO with TC $l = \pm 2$ [(a-1)–(d-1) and (a-2)–(d-2)] and $l = \pm 4$ [(a-3)–(d-3) and (a-4)–(d-4)], respectively, in the focal plane for different center angles α; the solid and dashed circles represent the phase singularity with $l = \pm 1$, respectively.

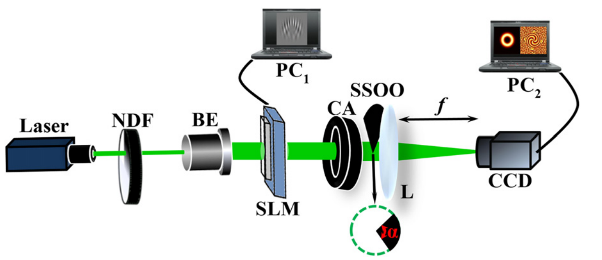

FIG. 5. Experimental setup for the generation of a Gaussian vortex beam obstructed by an opaque obstacle and the determination of its TC. NDF, neutral density filter; BE, beam expander; SLM, spatial light modulator; CA, circular aperture; SSOO, sector shaped opaque obstacle; L, thin lenses; PC_1 and PC_2, personal computers; and CCD, charge coupled device.

wavelength $\lambda = 532$ nm is first expanded by a beam expander (BE) and then modulated by the spatial light modulator (SLM) with forked gratings. The first-order diffracted beam, transmitted by a circular aperture (CA), generates a Gaussian vortex beam source. Then, this beam is focused onto the receiver plane by a thin lens L with focal length $f = 150$ mm and detected by a charge coupled device (CCD). A SSOO has been loaded on the source plane next to the CA. A neutral density filter (NDF) placed after the laser is used to adjust the strength of the incident laser beam. The personal computers (PC_1 and PC_2) were used to load the interference patterns and record the intensity distribution, respectively.

Figure 6 shows our experimental measurements of the normalized intensity distribution of the focused Gaussian vortex beam with $l = 4$ and $f = 150$ mm, obstructed by a SSOO with center angles $\alpha = 0°, 90°, 180°$, respectively, for different propagation distances z. The results demonstrate that the reconstructed intensity of a Gaussian vortex beam rotates 90° propagating from the source plane to the focal plane [see Figs. 6(a-2)–6(d-2) and 6(a-3)–6(d-3)]. The direction of rotation depends on the sign of the TC. The intensity distributions do not make it possible to determine the magnitude of the TC directly. Furthermore, we also perform the Fourier transform of the measured intensity patterns with $l = 2$, 3, and 4 in the focal plane, and the results are similar to those for the numerical results shown in Figs. 2(a-3), 2(c-3), and 2(d-3) for $\alpha = 0°$, 90°, and 180°, respectively. The magnitude of the TC cannot be obtained from the incomplete intensity distributions.

To verify our deduction that the reconstructed phase pattern can determine the magnitude and the sign of the TC, we measured the reconstructed phase distribution by the interference of OAM modes and plane waves. The reconstructed phase distribution of a focused Gaussian vortex beam with different TCs and different center angles α of the SSOO is shown in Fig. 7. One can infer from Fig. 7 that the phase variation direction determines the sign of the TC, such that the clockwise and counterclockwise directions correspond to the sign of the positive and negative TC, respectively. The number of phase singularities in the measured phase distributions denotes the magnitude of the TC even when the vortex beam has been obstructed by the SSOO with a center angle up to 180°. The experimental results agree well with the theoretical simulations.

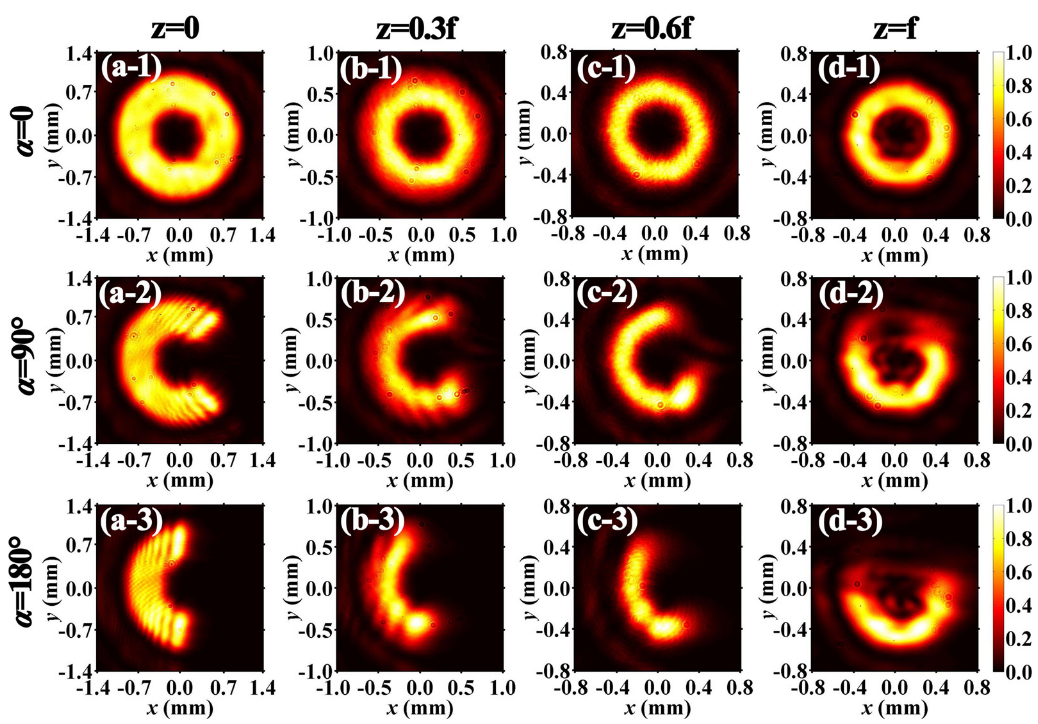

FIG. 6. Experimental measurements of the normalized intensity distribution of a focused Gaussian vortex beam with $l = 4$ and $f = 150$ mm, obstructed by a SSOO with center angles $\alpha = 0°$ [(a-1)–(d-1)], $\alpha = 90°$ [(a-2)–(d-2)], and $\alpha = 180°$ [(a-3)–(d-3)], respectively, for different propagation distances z.

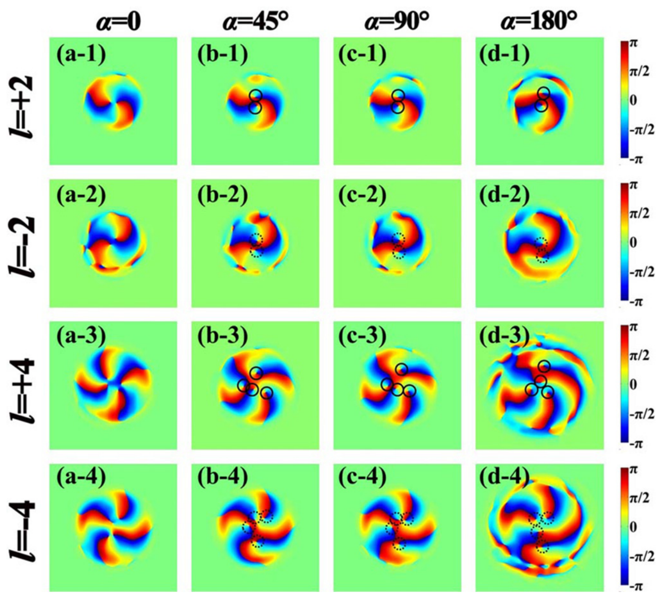

FIG. 7. Experimental measurements of the phase distribution of the Gaussian vortex beam with $f = 150$ mm obstructed by a SSOO with TC $l = \pm 2$ [(a-1)–(d-1) and (a-2)–(d-2)] and $l = \pm 4$ [(a-3)–(d-3) and (a-4)–(d-4)], respectively, in the focal plane for different center angles α; the solid and dashed circle represent the phase singularity with $l = \pm 1$, respectively.

In summary, we have numerically and experimentally investigated the intensity and phase evolution of a Gaussian vortex beam obstructed by a sector-shaped opaque obstacle. Our results clearly show that the reconstructed phase allows one to effectively determine the magnitude and sign of the TC of the obstructed vortex beam. The clockwise and anticlockwise movements of the spiral phase represent the positive and negative signs of the TC, respectively. The number of phase singularities corresponds to the magnitude of the measured TC. However, the information about the magnitude of the TC is lost based on the intensity measurement methods, e.g., Fourier transform of the far-field intensity patterns. Our findings enrich the methods for the measurement of the obstructed vortex beam's TC and will have found applications in OAM-based optical communications and optical trapping when obstacles in the optical path are inevitably encountered and the methods based on the intensity measurement are not feasible.

AUTHORS' CONTRIBUTIONS

All authors contributed equally to this work.

This work was supported by the National Natural Science Foundation of China (Grant Nos. 11974219, 91750201, 11525418, 11804198, 11904211, 11974218, and 91950104); the Shandong Provincial Natural Science Foundation of China (Grant Nos. ZR2019MA028 and ZR2019BA030); the Industry-University Cooperation Collaborative Education Project of the Ministry of Education of China (Grant No. 201902028023); the Innovation Group of Jinan (Grant No. 2018GXRC010); the Local Science and Technology Development Project of the Central Government (Grant No. YDZX20203700001766); and the China Postdoctoral Science Foundation (Grant No. 2018M642690).

DATA AVAILABILITY

The data that support the findings of this study are available from the corresponding author upon reasonable request.

REFERENCES

[1] L. Allen, M. W. Beijersbergen, R. J. C. Spreeuw, and J. P. Woerdman, Phys. Rev. A **45**, 8185 (1992).
[2] Q. Zhao, P. Yu, Y. Liu, Z. Wang, Y. Li, and L. Gong, Appl. Phys. Lett. **116**, 181101 (2020).
[3] A. E. Willner, H. Huang, Y. Yan, Y. Ren, N. Ahmed, G. Xie, C. Bao, L. Li, Y. Cao, Z. Zhao, 1J. Wang, M. P. J. Lavery, M. Tur, S. Ramachandran, A. F. Molisch, N. Ashrafi, and S. Ashrafi, Adv. Opt. Photonics **7**, 66 (2015).
[4] C. Zhang, C. Min, L. Du, and X. Yuan, Appl. Phys. Lett. **108**, 201601 (2016).
[5] H. He, M. E. J. Friese, N. R. Heckenberg, and H. Rubinsztein-Dunlop, Phys. Rev. Lett. **75**, 826 (1995).
[6] X. Li, H. Ma, H. Zhang, M. Tang, H. Li, J. Tang, and Y. Wang, Appl. Phys. Lett. **114**, 081903 (2019).
[7] A. Aleksanyan and E. Brasselet, Opt. Lett. **43**, 383 (2018).
[8] X. Li, Y. Tai, F. Lv, and Z. Nie, Opt. Commun. **334**, 235 (2015).
[9] S. Cui, B. Xu, S. Luo, H. Xu, Z. Cai, Z. Luo, J. Pu, and S. Chavez-Cerda, Opt. Express. **27**, 12774 (2019).
[10] G. C. G. Berkhout and M. W. Beijersbergen, Phys. Rev. Lett. **101**, 100801 (2008).
[11] P. Kumar and N. K. Nishchal, J. Opt. Soc. Am. A **36**, 1447 (2019).
[12] S. M. A. Hosseini-Saber, E. A. Akhlaghi, and A. Saber, Opt. Lett. **45**, 3478 (2020).
[13] J. Lu, C. Cao, Z. Zhu, and B. Gu, Appl. Phys. Lett. **116**, 201105 (2020).
[14] H. Gao, Y. Han, Y. Li, D. Zhu, M. Sun, and S. Yu, J. Opt. Soc. Am. A **35**, A40 (2018).
[15] S. Fu, T. Wang, Y. Gao, and C. Gao, Chin. Opt. Lett. **14**, 080501 (2016).
[16] J. Zhou, W. Zhang, and L. Chen, Appl. Phys. Lett. **108**, 111108 (2016).
[17] Z. Liu, S. Gao, W. Xiao, J. Yang, X. Huang, Y. Feng, J. Li, W. Liu, and Z. Li, Opt. Lett. **43**, 3076 (2018).
[18] Y. Li, Y. Han, and Z. Cui, IEEE Photonics Technol. Lett. **32**, 101 (2020).
[19] Y. Li, Y. Han, Z. Cui, J. Wang, and W. Zhao, J. Phys. D: Appl. Phys. **53**, 085106 (2020).
[20] L. A. Melo, A. J. Jesus-Silva, S. Chávez-Cerda, P. H. S. Ribeiro, and W. C. Soares, Sci. Rep. **8**, 6370 (2018).
[21] P. Zhao, S. Li, X. Feng, K. Cui, F. Liu, W. Zhang, and Y. Huang, Opt. Lett. **42**, 1080 (2017).
[22] H. Zhou, D. Fu, J. Dong, P. Zhang, D. Chen, X. Cai, F. Li, and X. Zhang, Light-Sci. Appl. **6**, e16251 (2017).
[23] C. Guo, S. Yue, and G. Wei, Appl. Phys. Lett. **94**, 231104 (2009).
[24] X. Lu, C. Zhao, Y. Shao, J. Zeng, S. Kongijnenberg, X. Zhu, S. Popov, H. P. Urbach, and Y. Cai, Appl. Phys. Lett. **114**, 201106 (2019).
[25] J. Zeng, X. Lu, L. Liu, X. Zhu, C. Zhao, and Y. Cai, Opt. Lett. **44**, 3881 (2019).
[26] H. Ma, X. Li, Y. Liang, Y. Tai, H. Li, J. Wang, M. Tang, Y. Wang, J. Tang, and Z. Nie, Opt. Lett. **42**, 135 (2017).
[27] M. Mazilu, A. Mourka, T. Vettenburg, E. M. Wright, and K. Dholakia, Appl. Phys. Lett. **100**, 231115 (2012).
[28] R. Liu, F. Wang, D. Chen, Y. wang, Y. Zhou, H. Gao, P. Zahng, and F. Li, Appl. Phys. Lett. **108**, 051107 (2016).
[29] V. V. Kotlyar, A. A. Kovalev, and A. P. Porfirev, Opt. Express **27**, 11236 (2019).
[30] L. Zhang, L. Zhang, and X. Liu, Phys. Rev. A **99**, 053606 (2019).
[31] P. Vaity, J. Banerji, and R. P. Singh, Phys. Lett. A **377**, 1154 (2013).
[32] S. Prabhakar, A. Kumar, J. Banerji, and R. P. Singh, Opt. Lett. **36**, 4398 (2011).
[33] Q. Zhao, M. Dong, Y. Bai, and Y. Yang, Photonics Res. **8**, 745 (2020).
[34] Y. Zhao, A. Wang, L. Zhu, W. Lv, J. Xu, S. Li, and J. Wang, Opt. Lett. **42**, 4699 (2017).
[35] G. Zhu, Y. Wen, X. Wu, Y. Chen, J. Liu, and S. Yu, Opt. Lett. **43**, 1203 (2018).
[36] S. li and J. Wang, Sci. Rep. **7**, 43233 (2017).
[37] J. Du and J. Wang, Opt. Lett. **40**, 4827 (2015).
[38] J. Durnin, J. Opt. Soc. Am. A **4**, 651 (1987).
[39] J. C. Gutiérrez-Vega, M. D. Iturbe-Castillo, and S. Chávez-Cerda, Opt. Lett. **25**, 1493 (2000).

[40]Z. Bouchal, J. Wagner, and M. Chlup, Opt. Commun. **151**, 207 (1998).
[41]F. Wang, Y. Chen, X. Liu, Y. Cai, and S. Ponomarenko, Opt. Express **24**, 23735 (2016).
[42]X. Liu, X. Peng, L. Liu, G. Wu, C. Zhao, F. Wang, and Y. Cai, Appl. Phys. Lett. **110**, 181104 (2017).
[43]F. O. Fahrbach, P. Simon, and A. Rohrbach, Nat. Photonics **4**, 780 (2010).
[44]M. McLaren, T. Mhlanga, M. J. Padgett, F. S. Roux, and A. Forbes, Nat. Commun. **5**, 3248 (2014).
[45]S. Vyas, M. Niwa, Y. Kozawa, and S. Sato, J. Opt. Soc. Am. A **28**, 1387 (2011).
[46]Q. Lin and Y. Cai, Opt. Lett. **27**, 216 (2002).
[47]E. Yao, S. F-Arnold, J. Courtial, S. Barnett, and M. Padgett, Opt. Express **14**, 9071 (2006).
[48]J. M. Hickmann, E. J. S. Fonseca, W. C. Soares, and S. Chavez-Cerda, Phys. Rev. Lett. **105**, 053904 (2010).
[49]O. Emile and J. Emile, Appl. Phys. B **117**, 487 (2014).
[50]D. Fu, D. Chen, R. Liu, Y. Wang, H. Gao, F. Li, and P. Zhang, Opt. Lett. **40**, 788 (2015).
[51]S. Zheng and J. Wang, Sci. Rep. **7**, 40781 (2017).
[52]D. Hebri, S. Rasouli, and A. M. Dezfouli, J. Opt. Soc. Am. A **36**, 839 (2019).